Effect of pre-shearing on the steady and dynamic rheological properties of mud sediments

Shakeel, Ahmad; Kirichek, Alex; Chassagne, Claire

DOI
10.1016/j.marpetgeo.2020.104338

Publication date
2020

Document Version
Final published version

Published in
Marine and Petroleum Geology

Marine and Petroleum Geology 116 (2020) 104338

Contents lists available at ScienceDirect

Marine and Petroleum Geology

journal homepage: www.elsevier.com/locate/marpetgeo

Research paper

Effect of pre-shearing on the steady and dynamic rheological properties of mud sediments

Ahmad Shakeel[a,b,*], Alex Kirichek[c], Claire Chassagne[a]

[a] Faculty of Civil Engineering and Geosciences, Department of Hydraulic Engineering, Delft University of Technology, Stevinweg 1, 2628 CN, Delft, the Netherlands
[b] Department of Chemical, Polymer & Composite Materials Engineering, University of Engineering & Technology, KSK Campus, Lahore, 54890, Pakistan
[c] Deltares, Boussinesqweg 1, 2629 HV, Delft, the Netherlands

ARTICLE INFO

Keywords:
Structural recovery
Mud sediments
Yield stress
Storage modulus
Two-step yielding

ABSTRACT

Mud sediments can exhibit a complex rheological behaviour particularly a thixotropic character or structural recovery after breakup due to the presence of organic matter/biopolymer. Such biopolymers can lead towards the development of flocculated structures having multiple length scales which are sensitive to shearing rate and history. In this study, the extent and rate of structural recovery of mud sediments was studied by measuring the storage modulus as a function of time using small amplitude oscillatory tests after a destructive steady shearing. This linear viscoelastic response of the sediments was further investigated as a function of several parameters including pre-shear rate, pre-shear time, measuring geometry, mud density and organic matter content. The equilibrium storage modulus (G'_∞) and the characteristic time (t_r) for the structural recovery of the sediment matrix were estimated by fitting the experimental data to a stretched exponential function. The normalized storage modulus, G'/G'_0 (i.e., structural parameter) was used to relate it with the yield stresses of mud sediments. The results showed that the recovery of structure after shearing was instantaneous (t_r being of the order of seconds), however, the extent of recovery was highly dependent on the studied parameters. The extent of recovery was higher for the samples with lower density and lower organic matter content. The effect of the shearing time on t_r and G'_∞ was almost negligible, which implies that the destruction of the structure was achieved within seconds. Using vane geometry, the extent of recovery was higher than using Couette geometry which is linked with the distribution of shear stresses within the cell for each geometry. Yield stresses showed a strong dependency on structural parameter, until it reaches very small values. At low values of structural parameter, the yield stresses were constant as the structural recovery was even faster than the time required to perform the amplitude sweep tests. This study provides an extensive knowledge about the structural recovery in mud sediments under different shearing conditions which can be useful for sediment management.

1. Introduction

Mud sediment contains clay, saline water, organic content and some amounts of silt and sand. It can exhibit rheological properties such as viscoelasticity, yield stress, shear-thinning (Nie et al., 2020; Shakeel et al., 2019, 2020) or, as will be shown in the present article, structural recovery after pre-shearing. The rheological analysis of mud sediments is essential to predict their transport properties (Mehta, 1986) because the rheological properties govern the response of mud to applied loads, resistance to deformation and flow and structural changes during shear (Berlamont et al., 1993).

Thixotropy is a (quasi-)reversible phenomenon. It is one of the very frequently observed complex rheological behaviours of the colloidal suspensions, in which the properties of the material are both time and shear rate dependent. Therefore, a material is typically stated as thixotropic if its viscosity displays a time dependency after the application of shear (stress) on an undisturbed sample and that the material displays a progressive recovery of this property after the removal of the applied shear (Mewis, 1979). This complex behaviour is usually observed in wide range of suspensions having dispersed particles of various shapes and sizes such as fibrous systems, foams, emulsions and polymeric materials (Cheng, 1987).

There are several methods to study the thixotropic behaviour of a system. Mewis and co-workers have determined the inherent drawbacks of using steady shearing methods to analyse the structural recovery of the system because in these methods the material's structure has to be

* Corresponding author. Faculty of Civil Engineering and Geosciences, Department of Hydraulic Engineering, Delft University of Technology, Stevinweg 1, 2628 CN, Delft, the Netherlands.
E-mail addresses: A.Shakeel@tudelft.nl (A. Shakeel), Alex.Kirichek@deltares.nl (A. Kirichek), C.Chassagne@tudelft.nl (C. Chassagne).

https://doi.org/10.1016/j.marpetgeo.2020.104338
Received 8 December 2019; Received in revised form 7 February 2020; Accepted 29 February 2020
Available online 05 March 2020

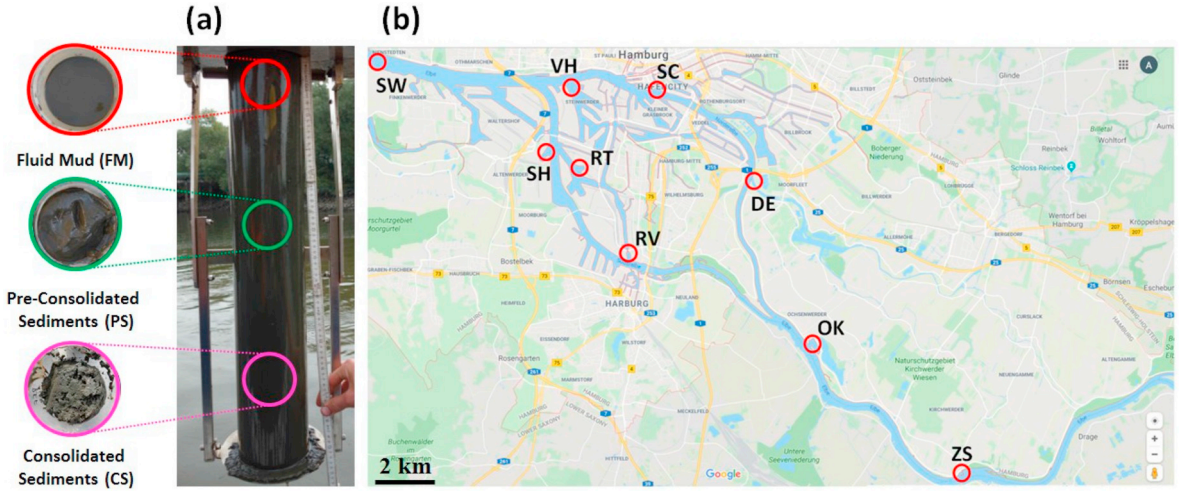

Fig. 1. (a) Sample collector of mud sediments (b) selected locations in the Port of Hamburg (Germany) to collect mud samples.

disturbed in order to be probed during the recovery phase (Schoukens and Mewis, 1978). Mewis and de Bleyser (1972) have shown that one can study the structural recovery of a polyamide gel in linseed oil by performing oscillatory measurements (i.e., non-destructive) within the linear viscoelastic regime of the material. This linear viscoelastic method has, henceforth, been used to analyse the rate and extent of structural recovery after steady or large amplitude oscillatory shearing for a variety of materials such as polymeric solutions (Janssens et al., 2017), pickering emulsions (Whitby and Garcia, 2014), slurries (Phuoc et al., 2014), cement pastes (Roussel et al., 2012), nanocomposite systems (Mobuchon et al., 2007), emulsion gels (Sun and Zhang, 2015) and synthetic colloidal dispersions (Mobuchon et al., 2009). The rate and extent of this structural recovery can be expressed in terms of thixotropy at a given kinematical condition (Mewis and de Bleyser, 1972).

Large amplitude oscillatory shear (100% strain) was used to break the structure of ferric oxide suspensions in mineral oil followed by the evolution of structure after the release of applied strain (Kanai et al., 1992). The extent and rate of structural recovery was observed to depend on the interactions between the particles and the concentration of the suspensions. Kinloch et al. (2002) examined the structural evolution in aqueous nanotube dispersions. The highly concentrated suspension recovered its initial storage and loss moduli within 1.5 h. Similar structural recovery was also described by Derec et al. (2003) and Coussot et al. (2006) for colloidal silica suspensions and pastes within linear viscoelastic regime upon cessation of shearing. The results showed (i) that the material behaves like a solid below yield stress but with irreversible deformations over long time periods and (ii) a structural recovery phenomenon (i.e., logarithmic increase in modulus) as a function of rest time above yield stress.

The growth of floc size and viscosity as a function of pre-shearing for different synthetic flocculated systems was studied in detail (He et al., 2012; McMinn et al., 2004; Xu et al., 2010). He et al. (2012) reported the temporal evolution of floc size and structure as a function of shear for flocculated kaolinite suspensions using polyaluminum chloride (PACl) as a coagulant. The results showed an increase in floc size as a function of shear rate (i.e., aggregation) in the initial stage followed by a plateau at 3 s^{-1} of shear rate and then a decline in floc size at higher shear rates (11-16 s^{-1}) due to the irreversible breakage of flocs. The effect of extracellular polymer (EPS) extraction from activated sludge on the time evolution of storage modulus was also investigated in the literature (Yuan et al., 2014). It was observed that the extraction of loosely bound EPS from the activated sludge resulted in higher elasticity (i.e., better structure) as a function of time. The floc size for muddy sediments or for sand/mud mixtures has also been analysed in the literature (Manning et al., 2010, 2011; Mehta et al., 2014; Soulsby et al., 2013; Spearman et al., 2011; Spencer et al., 2010; Whitehouse and Manning, 2007; Whitehouse et al., 2000). It is also reported in literature that the small amounts of organic matter can significantly affect the cohesiveness and rheological properties of muddy sediments (Malarkey et al., 2015; Parsons et al., 2016; Paterson et al., 1990; Paterson and Hagerthey, 2001; Schindler et al., 2015; Shakeel et al., 2019).

From the literature overview that we performed, it appeared that even though the thixotropic behaviour of synthetic suspensions (i.e., well-characterized clays in the presence of flocculating agents) has extensively been studied, the structural evolution of natural sediments has not been investigated. This probed us to investigate the following: (i) the structural breakup and recovery of mud sediments using small deformation rheology (i.e., by recording storage modulus as a function of time), (ii) the effect of several parameters including pre-shear time, pre-shear rate, temperature, sediment density, organic matter content, geometry of rheometer and oscillation frequency on the structural recovery of mud sediments, and (iii) the influence of pre-shear rate on the yield stresses of the sediments.

2. Materials and methods

2.1. Samples

In this study, the “undisturbed” mud samples were collected from different locations of Port of Hamburg (Germany) using 1 m core sampler (Fig. 1a). Fig. 1b shows the selected locations of the port with the associated names. The selected locations were chosen on the basis of a preliminary analysis, in order to have varying organic matter content. The cores were divided into different layers based on the differences in their visual consistency, ranging (as a function of depth) from fluid mud (FM), pre-consolidated (PS), pre-consolidated to consolidated (PS/CS) and consolidated (CS) sediment layers. Pre-consolidated sediments (PS) from RT location were used in this study for the detailed thixotropic (i.e., structural recovery) analysis because of their average density (compared to all locations) and minimum sedimentation problem (i.e., stable sample). The samples were packed in a sealed container and transported to the laboratory. The studies of the effect of mud density on the structural recovery behavior were performed using different mud layers collected from RT location (Table 1). The dry density of the sediments was taken to be about 2650 kg/m^3, following literature (Coussot, 1997). The bulk density of the sediments was determined by the oven drying method reported elsewhere (Coussot, 1997). The particle size distribution of the mud sediments was measured by using

Table 1
Characteristics of the different mud layers collected from RT location.

Sample ID	Density (kg/m^3)	TOC (% TS[b])	D_{50} (μm)
RT_PS	1228	3.9	15.2
RT_PS/CS	1258	3.7	20.2
RT_CS	1282	3.8	20.7

[b] TS = total solids

static light scattering, see Fig. 2a and b. The mud sample from SW location showed the highest D_{50} value (Table 2) and a bimodal particle size distribution which was linked with the presence of significant amount of sand. The organic matter content of the sediments was determined using an ISO standard 10694:1996–08 (ISO, 1995). The characteristics of the PS samples from different locations are summarized in Table 2. Before the rheological experiments, all the samples were homogenized by mild hand stirring.

2.2. Experimental protocol

Rheological experiments were performed using a HAAKE MARS I rheometer (Thermo Scientific, Germany) with concentric cylinder (Couette) geometry (CC25DIN, gap width = 2 mm and distance from the bottom of cup = 5.3 mm) and vane geometry (FL22, gap width = 5 mm and distance from the bottom of cup = 1 mm). The temperature was maintained at a desired value during each experiment using a Peltier controller system. Each experiment was carried out in duplicate and the repeatability error was always less than 2% (see Table 2 in supplementary information). In order to check the wall slip phenomenon, which is quite common for concentrated suspensions analysed by smooth geometries (Barnes, 1995), grooved Couette geometry was also used. The results of stress ramp-up test for smooth and grooved Couette geometries were in close agreement (data not shown) which showed the absence of wall slip. The pictorial representation of experimental protocol is shown in Fig. 3.

Initially, a resting time was allowed for each sample to ensure the reproducible state of the samples and to measure the initial structure level of the samples before shearing. Since the continuous phase (i.e., water) of the samples is Newtonian, the elastic character came from the presence of particles and flocs. Therefore, the storage modulus is an appropriate parameter to assess the structural level in the suspensions. Furthermore, it should be noted that the small amplitude time sweep experiments are non-destructive and thus the evolution of structure can be recorded in the almost absence of shear forces (i.e., almost at rest conditions).

Table 2
Characteristics of the pre-consolidated (PS) mud samples collected from different locations.

Sample ID	Density (kg/m^3)	TOC (% TS)	D_{50} (μm)
SW	1393	1.8	38.1
RT	1228	3.9	15.2
VH	1180	3.1	15.2
SC	1248	3.0	19.8
SH	1227	3.5	17.4
RV	1148	5.7	21.2
DE	1193	4.1	23.0
OK	1151	6.8	26.4
ZS	1235	4.6	25.9

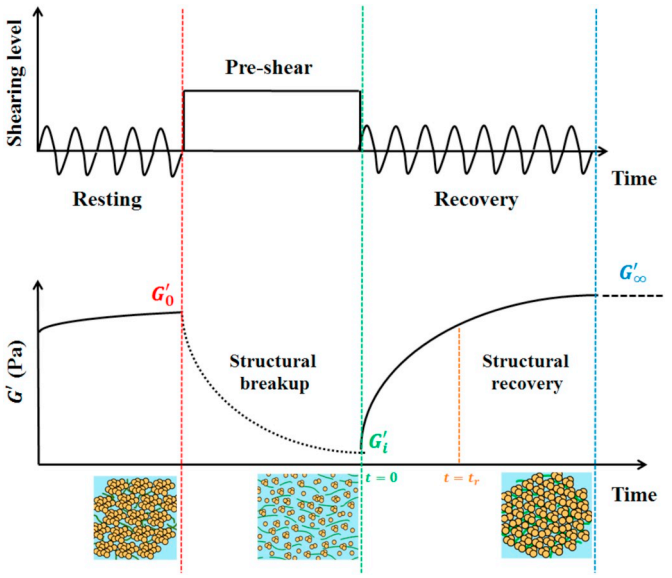

Fig. 3. Schematics of the experimental protocol employed for the structural breakup and recovery in mud samples.

In the first step of the experimental protocol, a resting time of 3–5 min was given before all the experiments after reaching the measurement position to eliminate the disturbances created by the measuring geometry. To estimate the storage modulus before the structural breakup, oscillatory time sweep within linear viscoelastic (LVE) regime at 1 Hz was performed. Preliminary amplitude sweep tests were also performed to determine the linear viscoelastic (LVE) regime. It was

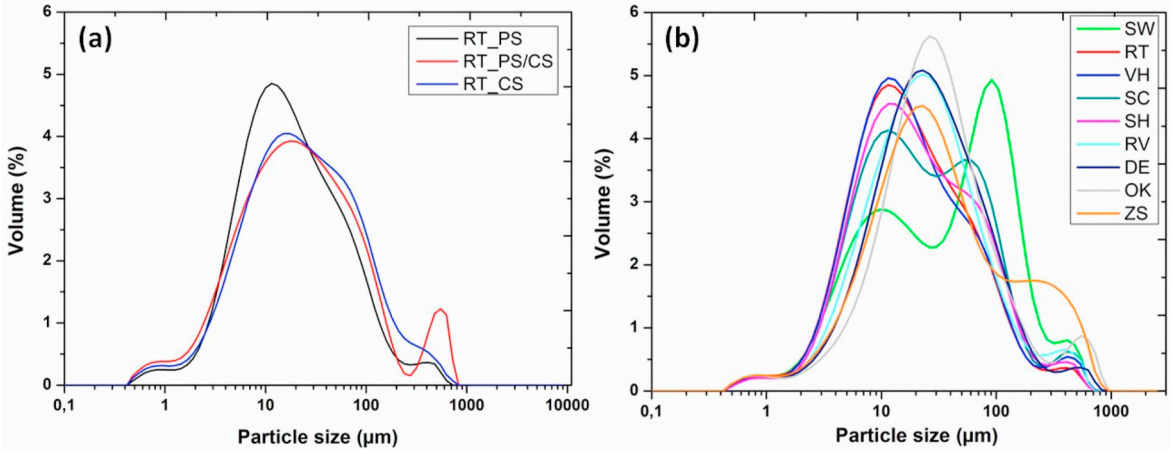

Fig. 2. Particle size distribution of (a) different mud layers from RT location and (b) pre-consolidated (PS) sediments from different locations obtained using static light scattering technique.

found that the resting time was long enough for all the samples to attain the constant storage modulus values (i.e., plateau). The storage (G') and loss (G'') moduli, obtained from oscillatory experiments, are the in-phase and out-of-phase responses of the material, respectively, to the applied sinusoidal stress/strain.

A steady pre-shearing step (second step in the protocol) was then performed to destroy the structure of the sediments. Preliminary studies were performed to investigate the effect of two different shearing modes (oscillating and steady) on the structural breakdown and recovery in mud sediments (see supplementary information). The higher structural breakdown was found in the case of steady shearing. In this article, results obtained with steady shearing are only presented.

The pre-shear rate values can have a significant effect on the structural evolution, thus, different pre-shear rates, ranging from 5 to 100 s^{-1}, were chosen to study the recovery of the structure as function of these shear rates. These shear rates were selected to have lower, intermediate and higher shearing action, based on a preliminary analysis. The shearing step was performed for 800 s. It was observed that this time was long enough for the viscosity (measured during this same period) to reach a constant value. This implies that the system has reached a steady-state structure.

Apart from pre-shear rate, it is also useful to investigate the effect of pre-shear duration on the structural regrowth of the mud sediments. Shearing steps were performed at two different pre-shearing rates (10 s^{-1} and 30 s^{-1}) by varying the pre-shearing duration from 10 to 800 s. The pre-shearing rates were selected to analyse the effect of pre-shearing time for two specific cases: (i) 10 s^{-1}, for which $G'_{\infty}/G'_0 > 1$ and (ii) 30 s^{-1}, for which $G'_{\infty}/G'_0 < 1$.

The third step of the protocol was the structural recovery of sediments, after the pre-shearing step. An oscillatory time sweep experiment was performed within the LVE regime to recover the structure with minimal disturbance. The amplitude of the oscillations, to have LVE regime, was determined by performing amplitude sweep experiments immediately after the pre-shearing step. The stress amplitude was selected within the LVE regime, for the recovery step (see supplementary information). The recovery step was performed for an interval of 500 s, which was long enough to capture the significant part of the structural recovery in mud sediments (see supplementary information). Preliminary studies were also performed to select the suitable frequency of oscillation for the recovery step. The results showed that a frequency of 1 Hz was the most suitable for the considered mud sediments (see supplementary information). The influence of temperature on the structural recovery was also studied by performing measurements at 5 and 25 °C. The results showed a higher structural recovery at the temperature of 25 °C (see supplementary information) and, therefore, this temperature was selected for the detailed analysis of structural recovery.

The equilibrium storage modulus (G'_{∞}) and the characteristic time (t_r) for the structural recovery of the sediment matrix was estimated by fitting the experimental data to a stretched exponential function. The stretched exponential function was adapted from Mobuchon et al. (2007, 2009) and reads as follows:

$$\frac{G'}{G'_0} = \frac{G'_i}{G'_0} + \left(\left(\frac{G'_{\infty} - G'_i}{G'_0}\right)\left(1 - \exp\left[-\left(\frac{t}{t_r}\right)^d\right]\right)\right) \quad (1)$$

where G' is the time dependent storage modulus of suspensions after shearing, G'_0 is the storage modulus before structural breakup, G'_i is the storage modulus right after pre-shearing (i.e., first value of the storage modulus obtained in the recovery step at t→0) and G'_{∞} is the equilibrium storage modulus as t→∞; t_r is the characteristic time of the material and denotes the rate of structural build-up (i.e., the time required for the system to attain 63% of its final value, G'_{∞}); d is the stretching exponent which reflects the sensitivity of the storage modulus on time (smaller value of d means faster recovery of storage modulus initially and slower at the later period) and its value lies within the range of 0–1. The fitting parameters in Eq. (1) are G'_{∞}, t_r and d.

In order to link the structural parameter (G'/G'_0) with yield stresses, amplitude sweep tests within the range of 0–250 Pa at a constant frequency of 1 Hz were performed after the recovery steps of different durations in the range $G'_i < G' < G'_{\infty}$. The effect of pre-shear rate on the apparent viscosity was also analysed by carrying out a shearing step followed by a stress ramp-up test at a rate of 1 Pa/s (without measuring steady state viscosity).

3. Results and discussion

3.1. One location: effect of pre-shear rate and pre-shear time

3.1.1. Effect of pre-shear rate

The structural recovery in sediment suspensions, after the structural breakdown caused by high shearing, was analysed by performing time sweep oscillatory experiments at very small amplitudes and recording the storage modulus of the suspensions as a function of time, as detailed in the experimental protocol section.

The structural evolution in terms of normalized storage modulus (i.e., with respect to the initial storage modulus G'_0) as a function of time is shown in Fig. 4a for different pre-shearing rates. An oscillating modulus response was obtained in some cases (Fig. 4a) in particular for concentrated sediments which have been sheared at lower shear rates. However, the normalized loss modulus (G''/G''_0), presented in Fig. 4b, shows the reduction in oscillating behaviour with time. The same type of oscillations have also been observed in the literature for polymeric solutions and synthetic suspensions, at the beginning of creep experiments, due to the elasticity of material. These oscillations also tend to disappear/minimize at longer experimental times (Goudoulas and Germann, 2016; Joshi et al., 2007). Therefore, the observed oscillations may be due to the elastic nature of the investigated samples.

It can be seen from Fig. 4a that for low shear rates, a better recovery was obtained. Eq. (1) was used to fit the data. The fitting parameters are presented in Table 3. Two important parameters, G'_{∞}/G'_0 and t_r are plotted as a function of pre-shear rate in Fig. 4c. It is interesting to note that both parameters displayed a decreasing trend with increasing shear rate till the shear rate of 35 s^{-1}, and is followed by an increase in both parameters for higher shear rates. This peculiar behaviour of equilibrium structure as a function of pre-shear rate was also observed in literature for synthetic suspensions of fumed silica and ferric-oxide (Kanai and Amari, 1993; Raghavan and Khan, 1995). The increase in floc size by increasing the shear rate was also observed in case of titanium tetrachloride ($TiCl_4$), ferric chloride ($FeCl_3$) and aluminum sulfate ($Al_2(SO_4)_3$) flocs (Zhao et al., 2013).

A possible explanation for this peculiar behaviour is presented in Fig. 5. The initial structure (Fig. 5a) is composed of an interconnected network of sediment-rich flocs along with polymer chains (i.e., organic matter). The bonds most prone to fail at shearing will be at the junction points between flocs. Therefore, at low pre-shear rates, it is believed that these bonds will break leading to an alignment of the polymer chains (Fig. 5b). After shearing, it is assumed that the flocs will form a weaker interconnected network (with more open spaces) and have less junction points (Fig. 5c). With time, some strength will be recovered as a result of the reformation of the organic matter-flocs bonds. Nonetheless, the floc structure remains less interconnected as at the start, implying $G'_{\infty}/G'_0 < 1$.

At very higher shear rates, in addition to the breakdown of the interconnected network of flocs, it is thought that the breaking or recoiling of individual flocs into smaller flocs along with the scission and/or re-conformation of polymer chains could also occur (Fig. 5b). After shearing, it is expected that these smaller entities (flocs, particles and polymer chains) are able to interact in such a way that a better interconnected network is created. For the largest shear rate of 100 s^{-1}, the equilibrium structural parameter (G'_{∞}/G'_0) was then even larger than 1

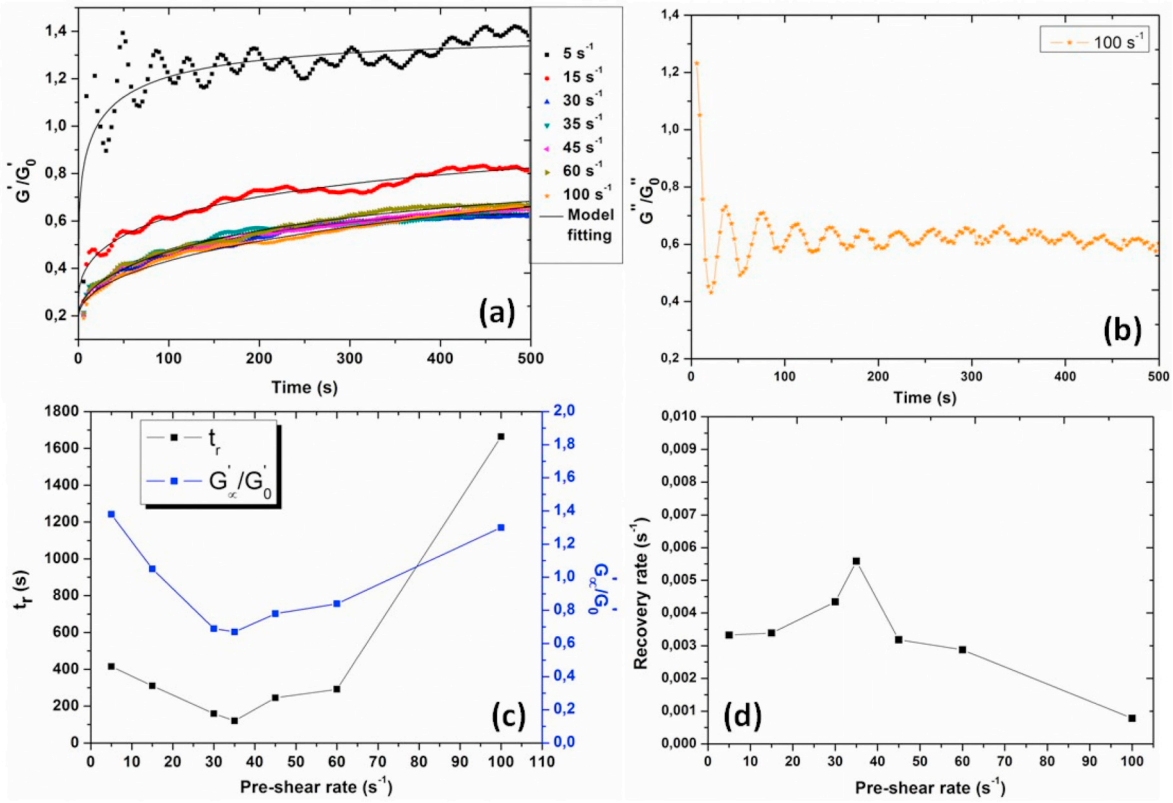

Fig. 4. (a) Normalized storage modulus (G'/G_0') as a function of time for different pre-shear rates using RT sediments, solid line represents model fitting, (b) normalized loss modulus (G''/G_0'') as a function time for 100 s^{-1} using RT sediments, the solid line is just a guide for the eye, (c) model parameters as a function of pre-shear rate, the solid line is just a guide for the eye, (d) recovery rate $\left(\frac{G_\infty'/G_0'}{t_r}\right)$ as a function of pre-shear rate for RT sediments, the solid line is just a guide for the eye.

Table 3
Values of the model parameters for different pre-shearing rates.

Pre-shear rate (s^{-1})	G_∞' (Pa)	G_∞'/G_0'	t_r (s)	d (−)	r^2 (−)
5	3255	1.38	415	0.37	0.57
15	2068	1.05	310	0.46	0.96
30	1527	0.69	159	0.67	0.99
35	1388	0.67	120	0.67	0.99
45	1606	0.78	245	0.58	0.99
60	1646	0.84	292	0.59	0.99
100	2644	1.30	1664	0.50	0.99

(Table 3). This hypothesis of a densification of the network after shearing, when the interconnected structure has been broken in small entities, has in fact been predicted and experimentally observed in literature (Van Den Tempel, 1979).

The time to reach 63% of G_∞' (i.e., t_r) is shown in Fig. 4c as a function of pre-shear rate. As for the equilibrium structural parameter (G_∞'/G_0'), at low pre-shear rates (< 35 s^{-1}), a decrease in recovery time (t_r) with increasing shear rate was also observed whereas a significant increase at higher shear rates was found. By applying smaller shear rates, as already explained previously (Fig. 5), the breakage of individual flocs is supposed not to be significant which is in accordance with smaller recovery times. As increasing the shear rate (below 35 s^{-1}) led to a lesser recovery, the recovery rate (see Fig. 4d) was increasing as a function of shear rate. At high shear rates (above 35 s^{-1}), the breakdown of flocs was thought to be more pronounced with increasing shear rate which corresponded to a higher recovery time, a better recovery ($G_\infty'/G_0' > 1$) and consequently a lower recovery rate. The similar increase in characteristic time as a function of increasing pre-shearing rate was also observed for MWCNTs based suspension in epoxy, by recording storage modulus as a function of time after pre-shearing and fitting the data to an exponential function (Khalkhal et al., 2011).

3.1.2. Effect of structural recovery time on yield stresses

In natural environments, shear rates are time-dependent, and it is quite often so that the systems are not at full recovery. During the recovery phase, inter-particle forces will lead to the development of strength within the material structure. These natural systems therefore have time dependent yield stress and viscoelastic properties (Barnes, 1999).

This time dependence was investigated by correlating the structural parameter (G'/G_0'), at a specific recovery time 't', with its corresponding yield stresses (Fig. 6a). The pre-shear rate was taken to be 30 s^{-1} and was applied for 800 s. Fig. 6b displays the outcome of the amplitude sweep tests performed after different recovery times, i.e., for different G'/G_0' values. The value, $G'/G_0' = 1$, corresponds to an experiment whereby the amplitude sweep test was performed right after the resting time (no pre-shear was applied). Two distinct declines (i.e., two-step yielding) in the storage modulus values were observed, associated to "static" and "fluidic" yield stresses, according to the terminology used by (Shakeel et al., 2020). The yield stresses were linked to the breakage of the interconnected network into large flocs (static yield stress) and the further breakage of these flocs into very small aggregates or individual particles (fluidic yield stress) (Fig. 6c), much in line with the conceptual picture displayed in Fig. 5. One can see that regardless of the recovery time, two yield stresses (i.e., two-step yielding) were always observed. This implies that even at very small recovery times (i.e. just after pre-shearing) the structure reforms at a macroscale.

The correlation between the structural parameter (G'/G_0') and the yield stresses is shown in Fig. 6d. It is clearly evident from the figure

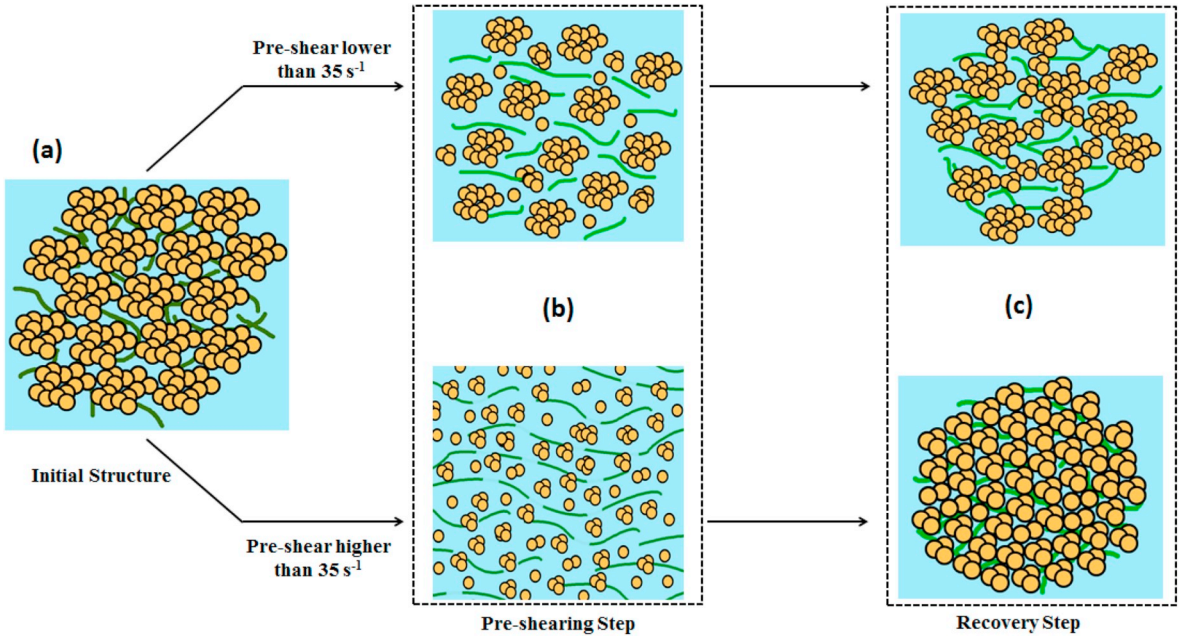

Fig. 5. Schematic illustration of structural breakup and recovery at lower ($< 35\ s^{-1}$) and higher ($> 35\ s^{-1}$) pre-shear rate (a) initial structure, structural changes during the (b) pre-shearing step, and (c) recovery step.

that the yield stresses show a sharp decline with decreasing structural parameter up to $G'/G'_0 = 0.5$ and the yield stress values remained more or less constant for $G'/G'_0 < 0.5$. For $G'/G'_0 < 0.5$, i.e. at small recovery times, both yield stresses were independent of the recovery time (i.e., structural parameter), which implies that the restructuring within the sample at micro and macroscale was faster than the experimental time of the amplitude sweep (150–170 s). The values of the yield stresses were lower, implying that the micro and macro structures have not fully

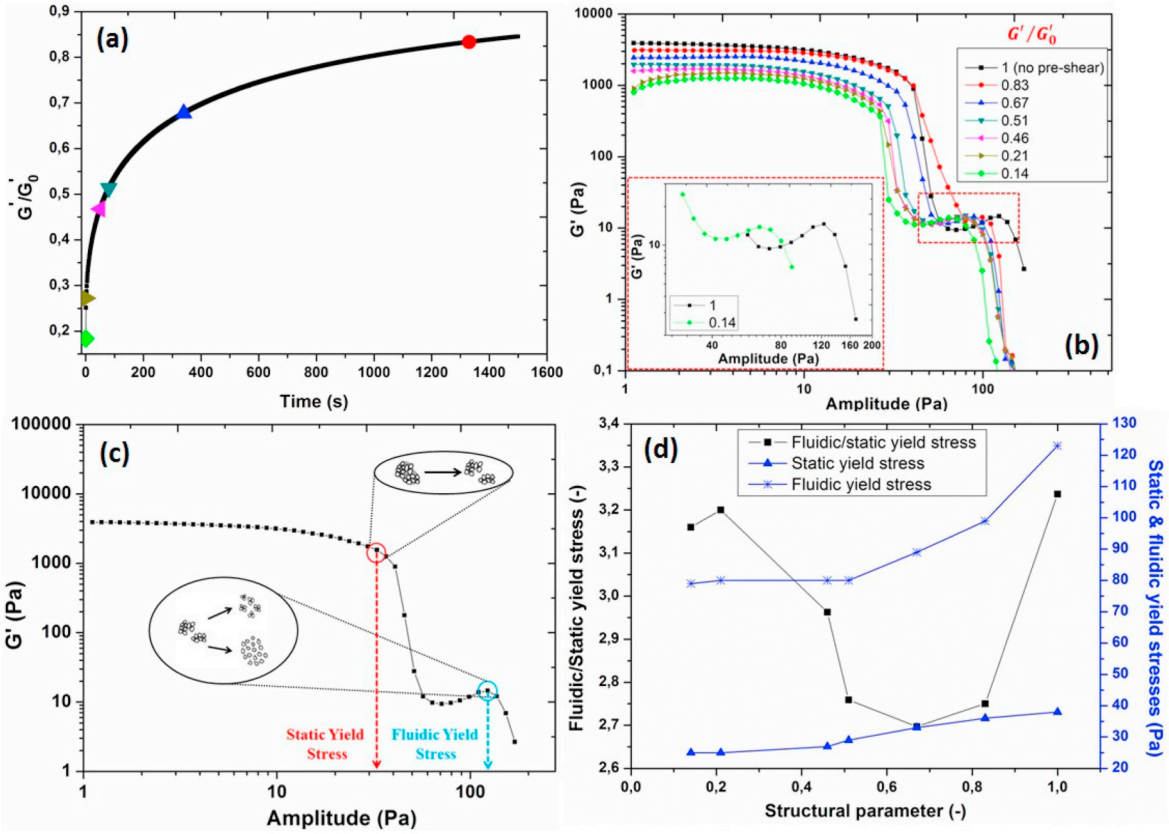

Fig. 6. (a) Schematic representation of structural recovery step with different values of structural parameter, different colored points represent the selected recovery times to perform amplitude sweep tests afterwards, (b) storage modulus as a function of amplitude for different values of structural parameter (G'/G'_0) using RT sediments, (c) schematic representation of static and fluidic yield stress values in oscillatory amplitude sweep tests (d) correlation between structural parameter and static, fluidic and fluidic/static yield stress values of RT sediments, the solid line is just a guide for the eye.

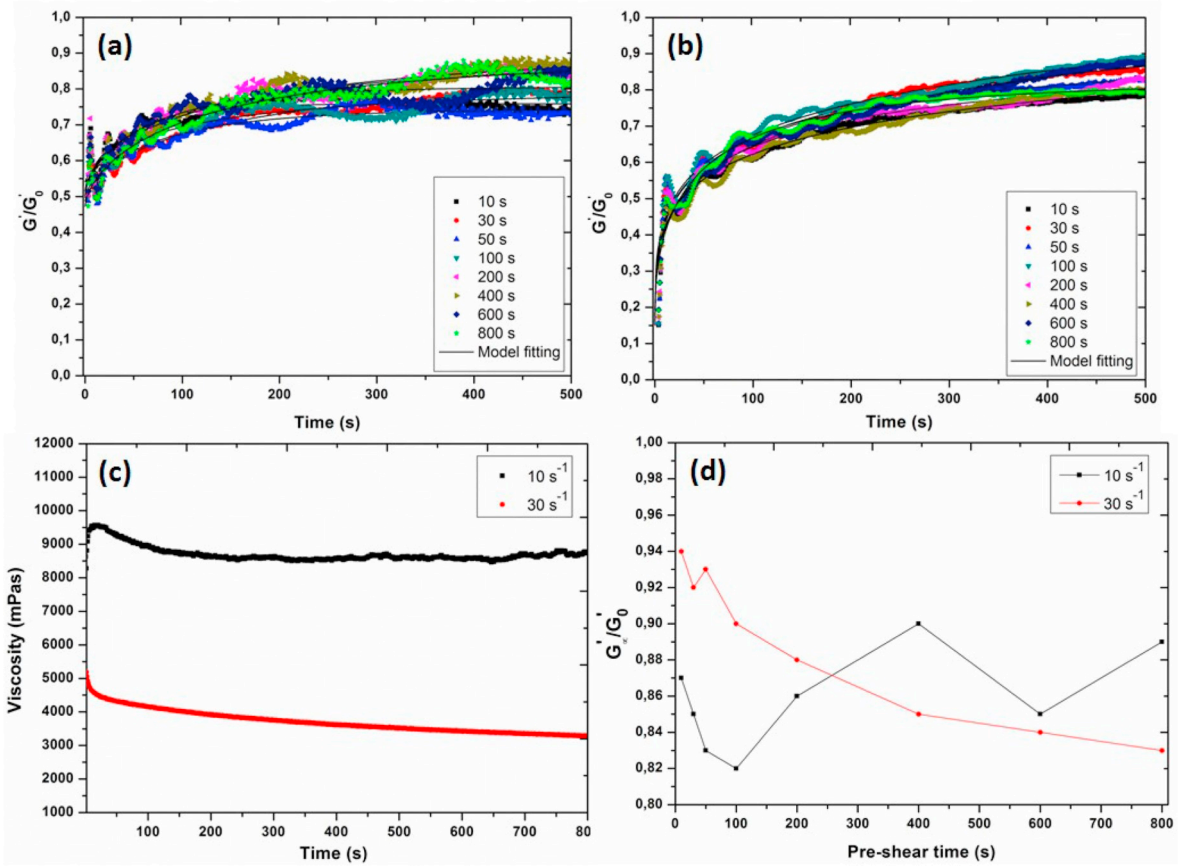

Fig. 7. Normalized storage modulus (G'/G'_0) as a function of time for different pre-shearing times using RT sediments pre-sheared at (a) 10 s^{-1} and (b) 30 s^{-1}; (c) viscosity as a function of time for different pre-shear rates during the shearing step using Couette; (d) equilibrium structural parameter (G'_∞/G'_0) as a function of pre-shear time for different pre-shear rates.

recovered. For higher recovery times, both static and fluidic yield stresses increased as function of the structural parameter, indicating that the stronger the microstructure, the stronger the macrostructure. This is also in line with the conceptual representation displayed in Fig. 5 for high pre-shear rates. It can be noted from Fig. 6d that the ratio of fluidic to static yield stress shows a decline with increasing structural parameter for $G'/G'_0 < 0.7$ and then a sudden increase for higher values of G'/G'_0. This may be linked with the fact that below the recovery time associated to $G'/G'_0 = 0.7$, smaller or individual flocs remain the same (i.e., same fluidic yield stress) while the interconnected network of individual flocs (which gives rise to the static yield stress) is changing.

On a side note, we also observed the existence of a jamming phenomenon in the outcome of the amplitude sweep tests, in terms of an increase in storage modulus values at higher stress amplitudes (see inset of Fig. 6b). Such type of shear thickening/jamming behaviour in oscillatory amplitude sweep tests was also observed for fumed silica and Aeorsil nanoparticles-based suspensions (Fischer et al., 2007; Galindo-Rosales et al., 2009).

3.1.3. Effect of pre-shear time

Fig. 7a and b shows the evolution of the structural parameter (G'/G'_0) as a function of time for different pre-shearing durations and for two pre-shear rates (10 and 30 s^{-1}). It was found that the influence of shearing duration on the structural evolution of the samples, for both shearing rates, was not very significant. As can be seen from Fig. 7c, the viscosity behaviour was, however, significantly different for these two cases. The model parameters of Eq. (1), presented in Tables 4 and 5, are also plotted as a function of pre-shearing time (Fig. 7d). For the lower pre-shear rate (10 s^{-1}), the equilibrium structural parameter (G'_∞/G'_0) was quite fluctuating as a function of pre-shearing time in the range [0.82–0.90] whereas for the higher pre-shear rate (30 s^{-1}), a decrease of G'_∞/G'_0 as a function of pre-shearing time was found from 0.94 (t = 10 s) to 0.82 (t = 800 s). These findings are in line with the schematic illustration shown in Fig. 5.

Yüce and Willenbacher (2017) investigated the effect of pre-

Table 4
Values of the model parameters for different shearing times at 10 s^{-1}.

Pre-shear time (s)	G'_∞ (Pa)	G'_∞/G'_0	t_r (s)	d (−)	r^2 (−)
10	2803	0.87	47	0.91	0.81
30	3030	0.85	145	0.72	0.94
50	2754	0.83	70	0.75	0.85
100	2947	0.82	90	0.57	0.82
200	3294	0.86	126	0.58	0.89
400	3371	0.90	160	0.62	0.90
600	2979	0.85	65	0.77	0.81
800	3270	0.89	131	0.66	0.94

Table 5
Values of the model parameters for different shearing times at 30 s^{-1}.

Pre-shear time (s)	G'_∞ (Pa)	G'_∞/G'_0	tr (s)	d (−)	r^2 (−)
10	2810	0.94	115	0.37	0.96
30	3349	0.92	262	0.34	0.96
50	2790	0.93	90	0.39	0.96
100	3919	0.90	460	0.32	0.96
200	2776	0.88	100	0.40	0.96
400	3283	0.85	254	0.34	0.98
600	3479	0.84	399	0.38	0.98
800	2470	0.83	54	0.54	0.97

shearing rate and time on the structural recovery of silver pastes. Their results revealed a strong dependency of the structural recovery on the pre-shear amplitude (i.e., lower recovery with higher pre-shear rate) whereas the recovery was not significantly affected by the pre-shear time. Similar results, i.e., structural recovery dependence on pre-shear rate and fairly independence of pre-shearing time was also observed for fumed silica suspensions and non-polar polymer/clay nanocomposites (Mobuchon et al., 2007; Raghavan and Khan, 1995).

At lower pre-shear rate (10 s^{-1}), the viscosity displayed an increase and then remained in good approximation constant as a function of time (Fig. 7c). However, at higher pre-shearing (30 s^{-1}), a continuous decrease in viscosity is observed. The observed overshoot in viscosity is related to the viscoelasticity of the material and it depends on the Deborah number (i.e., the ratio of relaxation to experimental time). At low Deborah number (De), a typical increase in transient viscosity is usually observed. By increasing De (i.e. increasing the shear rate), the overshoot moves towards lower times. At very high De values, the overshoot cannot be observed as the experimental time is too fast. A monotonous decrease in viscosity is then observed.

3.1.4. Effect of pre-shear on apparent viscosity

The influence of pre-shearing on the apparent viscosity of mud sediments was also investigated. The stress ramp-up experiments were performed immediately after the shearing step without the execution of any recovery step. Fig. 8a and b shows the results of stress ramp-up tests in terms of apparent viscosity as a function of stress for different pre-shearing rates and pre-shearing times, respectively. Two yield stresses, static and fluidic, were estimated from the two viscosity declines (Shakeel et al., 2020). These two characteristic declines of apparent viscosity in stress sweep experiments were also observed in the literature for artificial and natural suspensions (Habermann and Wurpts, 2008; Nosrati et al., 2011). A decrease in yield stress values were observed with increase in pre-shear rate or pre-shear time due to the enhanced structural breakdown.

The correlation between the yield stresses and pre-shear rate or pre-shear time is shown in Fig. 8c and d, respectively. The yield stress values displayed a decrease with increasing shear rate up to a certain level and after which the values remain in good approximation constant (Fig. 8c). This result may be linked with the results shown in Fig. 6d. As explained in the corresponding section, when the structure is fully broken, the initial recovery of both micro and macro structures is faster than the experimental time of the stress ramp-up test. The yield stress values showed a decreasing trend as a function of pre-shear time (Fig. 8d). This reflects the extensive structural breakdown as a function of increasing shear time, as was already shown in Fig. 7c. Shear jamming was also observed in the stress ramp-up experiments. This jamming occurred at higher stresses and decreased as a function of pre-shear rate (see inset of Fig. 8a). However, the jamming remains the same for different pre-shearing times at 30 s^{-1} (see inset of Fig. 8b).

3.2. Different locations: effect of sediment density, organic matter and geometry of rheometer

The effect of organic matter, sediment density and rheometer geometry (Couette and Vane) on the structural recovery in mud sediments was investigated. Several samples were collected from different locations of Port of Hamburg with varying organic matter content (Table 2). Fig. 9a and b shows the structural regrowth in mud sediments as a function of time for different samples pre-sheared at 100 s^{-1} for 800 s using Couette and Vane geometries, respectively.

Fig. 9a clearly shows that the sample with lowest organic matter content (SW) displays a higher recovery than the samples having higher

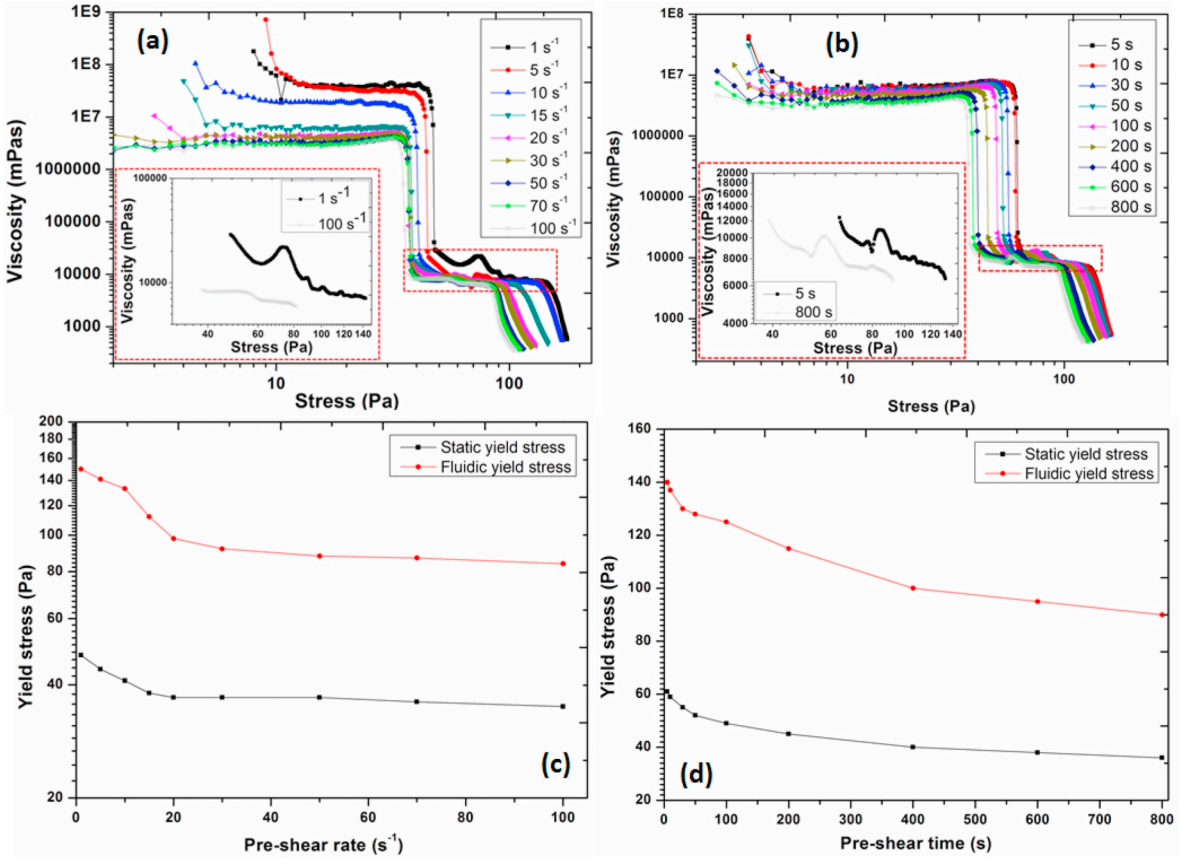

Fig. 8. Apparent viscosity as a function of stress using RT sediments for different (a) pre-shearing rates and (b) pre-shearing times; correlation of the yield stresses with the (c) pre-shearing rate and (d) pre-shearing time, the solid line is just a guide for the eye.

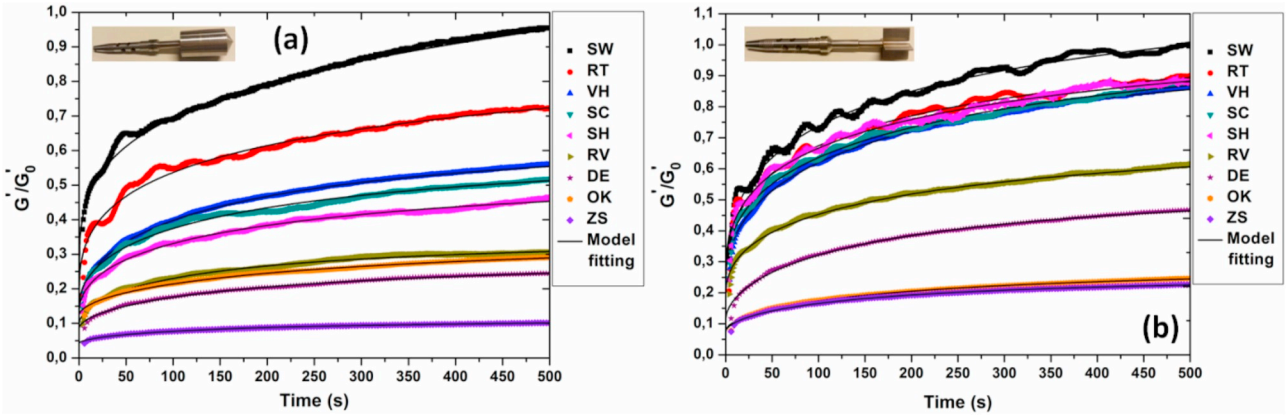

Fig. 9. (a) Normalized storage modulus (G'/G'_0) as a function of time for different pre-consolidated (PS) sediment samples pre-sheared at 100 s^{-1} using (a) Couette and (b) Vane geometries.

Table 6
Values of the model parameters for different sediment samples with Couette geometry.

Location	Density (kg/m^3)	G'_∞ (Pa)	G'_∞/G'_0	t_r (s)	d (−)	r^2 (−)
SW	1393	2380	1.13	343	0.75	0.99
RT	1228	3145	0.98	369	0.41	0.98
VH	1180	517	0.63	178	0.58	0.99
SC	1248	891	0.61	211	0.52	0.99
SH	1227	1177	0.55	229	0.51	0.99
RV	1148	533	0.34	147	0.59	0.99
DE	1193	273	0.29	235	0.61	0.99
OK	1151	237	0.35	313	0.59	0.99
ZS	1235	359	0.11	177	0.62	0.99

organic matter (ZS, OK, DE and RV). Furthermore, in the case of sediments from SW location, the equilibrium structural parameter (G'_∞/G'_0) was even higher than 1 (Table 6) with Couette geometry, which may be linked to the presence of higher amount of sand, (see particle size distribution of the sample from SW location in Fig. 2b). The shearing action is known to facilitate the settling of sand particles (Coussot, 1997). Because of the settling, a structure consisting of a majority of clay particles might be formed with a higher elasticity than the initial sediment sample (see Fig. 10). The settling of sand particles in sand-clay mixtures during flow and the resultant increase in yield stress values were reported in the literature (Ilstad et al., 2004).

The extensive shearing of the samples having higher amount of organic content may cause severe destruction/re-conformation of the polymeric chains which were not able to regain their initial state after cessation of shearing (i.e., smaller values of G'_∞/G'_0, Table 6). Therefore, a large amount of polymers in a suspension is not beneficial for the structural recovery phenomenon, as also reported in literature for flocculated bentonite suspensions (Hammadi et al., 2014Barbot et al., 2010) and kaolinite suspensions flocculated with aluminium sulfate hydrate (Yu et al., 2011).

Fig. 9b shows higher structural recoveries for the sediments pre-sheared using vane geometry. As can also be seen from Fig. 11a, the equilibrium structural parameter (G'_∞/G'_0) of the sediments pre-sheared by vane geometry was much higher than the one observed with Couette. With vane we get in general $G'_\infty/G'_0 > 1$ (see Table 7). This may be attributed to the fact that vane geometry is very effective in disturbing the macroscopic/bulk structure of the sample. During the recovery step, this bulk material can regrow to a stronger structure. In contrast, the pre-shearing using the Couette geometry leads to a more complete destructuration of the sample. The sample can only regrow to a stronger structure ($G'_\infty/G'_0 > 1$) for very specific conditions as discussed under Fig. 4c. This efficiency of the vane geometry to form highly structured samples has led to its utilization as a mixer for preparing polymeric blends with enhanced mechanical and structural properties (Qu et al., 2013; Xiaochun et al., 2015).

The effect of sediment density on the structural recovery was also investigated by analysing different sediment layers collected from same location, in order to have similar organic matter content (see Table 1).

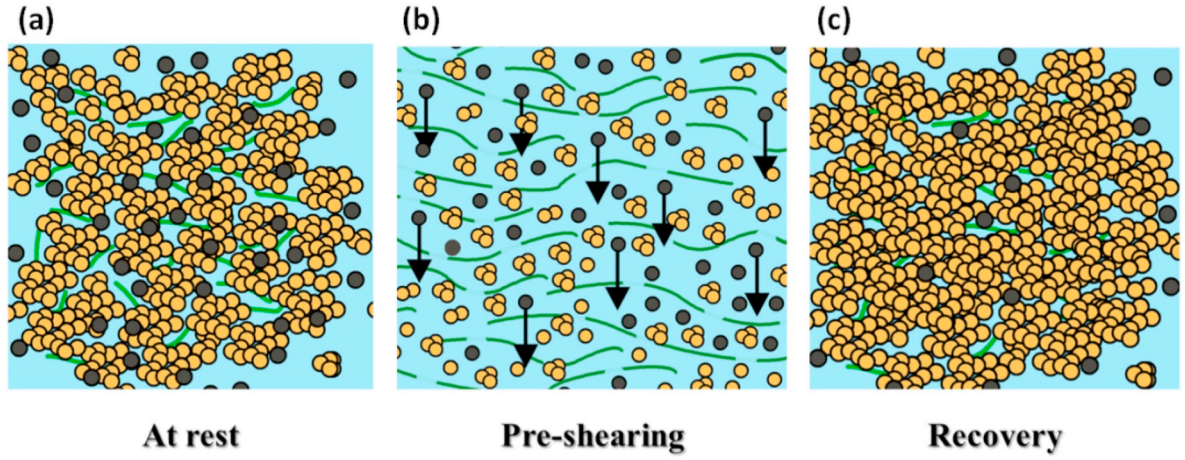

Fig. 10. Schematic illustration of structural breakdown and recovery in sediments from SW location (a) initial sample, (yellow circles represent clay particles), (b) structural changes during the pre-shearing step, black arrows represent the settling of sand particles (shown as black circles) during shearing action, (c) structural changes during recovery step. (For interpretation of the references to color in this figure legend, the reader is referred to the Web version of this article.)

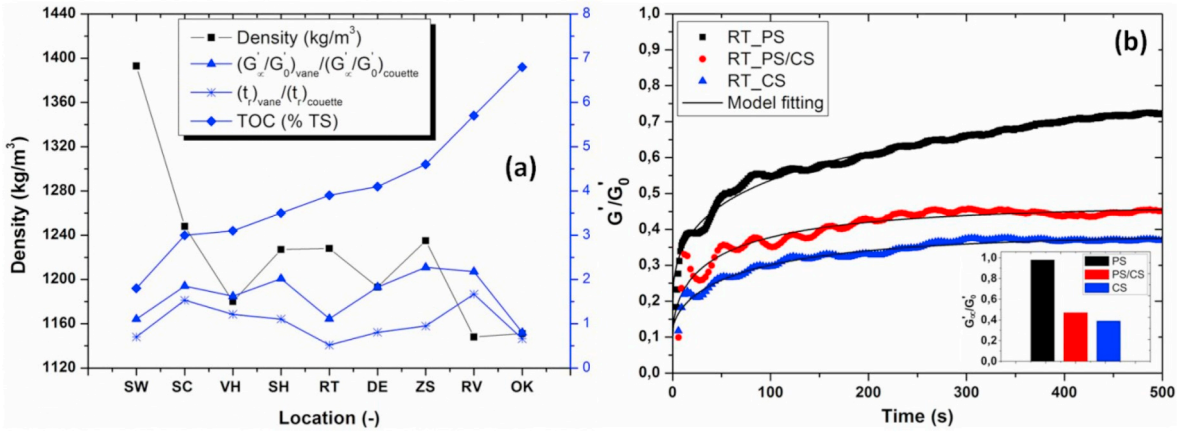

Fig. 11. (a) Density, $\frac{(G'_{\infty}/G'_0)_{vane}}{(G'_{\infty}/G'_0)_{couette}}$, $\frac{(t_r)_{vane}}{(t_r)_{couette}}$ and organic matter content (TOC) as a function of different locations, solid line is just a guide for the eye, (b) normalized storage modulus (G'/G'_0) as a function of time for different mud layers collected from RT location pre-sheared at 100 s^{-1} using Couette geometry. Inset shows the equilibrium structural parameter (G'_{∞}/G'_0) for different mud layers.

Table 7
Values of the model parameters for different sediment samples with Vane geometry.

Location	Density (kg/m^3)	G'_{∞} (Pa)	G'_{∞}/G'_0	t_r (s)	d (−)	r^2 (−)
SW	1393	7753	1.25	240	0.45	0.99
RT	1228	9506	1.09	192	0.43	0.98
VH	1180	2185	1.02	216	0.53	0.99
SC	1248	3937	1.13	323	0.46	0.99
SH	1227	4698	1.11	253	0.43	0.99
RV	1148	2467	0.74	245	0.49	0.99
DE	1193	1186	0.53	189	0.61	0.99
OK	1151	801	0.28	207	0.61	0.99
ZS	1235	1408	0.25	168	0.61	0.99

Table 8
Values of the model parameters for different sediment samples with Couette geometry.

Location	Density (kg/m^3)	G'_{∞} (Pa)	G'_{∞}/G'_0	t_r (s)	d (−)	r^2 (−)
RT_PS	1228	3145	0.98	369	0.41	0.98
RT_PS/CS	1258	5539	0.47	53	0.53	0.90
RT_CS	1282	12670	0.39	82	0.62	0.97

The results for different sediment layers from RT location are presented in Fig. 11b. The results displayed a decrease in recovered modulus values with the depth at which the samples were collected. This result is strongly correlated to the fact that the deeper the sediment, the higher the density. A high density leads to a higher structured network, which can be extensively disturbed by the shearing action. This also leads to lower structural recoveries in the sediments after the shearing step for higher sediment densities (i.e., smaller values of G'_{∞}/G'_0, see Table 8). As far as the characteristic time t_r is concerned, the effect of organic matter was not very significant on its value for both Couette and vane geometries. This implies that the vane geometry was useful in attaining stronger equilibrium structures of the sediments without affecting their characteristic recovery time (t_r).

This study was focused on the structural recovery in mud sediments after a steady pre-shearing action, which is quite different from the concept of thixotropy (i.e., continuous decrease in viscosity with shearing action and the subsequent recovery of viscosity in time when the applied shear is removed). However, both these approaches provide similar outcome regarding the thixotropic character of the sample.

From this study, it is found that the mud layer with lowest density (PS layer) displayed faster structural recovery than the one with highest density (CS layer). In our previous investigation (Shakeel et al., 2020), we found that for similar mud samples the area of thixotropic loop (upward and downward viscosity/stress curve) was very small for the mud sample with lowest density (FM layer). This behaviour can be related to a very fast recovery in structure for FM layers. The area of thixotropic loop for dense mud layers (CS layer), on the other hand, was quite significant implying a slower recovery (Shakeel et al., 2020).

The insight into the rheological behaviour of natural muddy sediments, in particular the effect of pre-shearing on structural recovery is very important. This has wide implications for a marine environment as this rheological behaviour will influence the mud resuspension behaviour, bed stability, erosion, sediment mixing, turbulence damping and also the ability to define navigable mud layers.

4. Conclusions

In this study, the structural recovery of mud sediments was investigated by varying different pre-shearing conditions. The structural recovery behaviour of a specific sample was first thoroughly studied. This sample, from the location named RT, was chosen because its density is representative of the mean density value of all samples and it has minimum sedimentation problem. The equilibrium structural parameter (G'_{∞}/G'_0) of the sediments obtained from the RT location displays an interesting behaviour as a function of pre-shearing rate with a minimum value at 35 s^{-1} and an increase in structural parameter after this pre-shear rate. This behaviour is linked with the existence of two structure levels (i.e., two-step yielding). Further (rheo-optical) studies are required to verify the validity of the proposed mechanism that is at the origin of this behaviour. The structural parameter (G'/G'_0) is observed to be strongly correlated to the yield stress values up to a certain value ($G'/G'_0 = 0.5$). Below this value of structural parameter, it is found that the structural recovery is faster than the time required to perform the dynamic amplitude sweep tests.

The equilibrium structural parameter (G'_{∞}/G'_0) is almost independent of shearing time but a higher structural recovery was obtained with vane geometry as compared to the Couette geometry. The highest values for equilibrium structural parameter (G'_{∞}/G'_0) are found for the sediments having the lowest density and lowest organic matter. The characteristic time of recovery (t_r) is found to be significantly affected by the pre-shear rate and temperature. Mud samples collected from different locations differ in organic matter content and densities. Further research work is required to analyse the effect of organic matter content (amount and type), for a given density, on the structural recovery of mud sediments. This study provides an extensive knowledge about the structural recovery in mud sediments as a function of

different pre-shearing conditions, which is critical from fundamental point of view as well as for industrial applications such as sediment management after dredging.

CRediT authorship contribution statement

Ahmad Shakeel: Methodology, Investigation, Formal analysis, Writing - original draft. **Alex Kirichek:** Conceptualization, Writing - review & editing, Project administration. **Claire Chassagne:** Supervision, Writing - review & editing, Formal analysis, Funding acquisition.

Declaration of competing interest

The authors declare that they have no competing financial interests or personal relationships that could influence the results reported in this paper.

Acknowledgements

This study is funded by the Hamburg Port Authority and carried out within the framework of the MUDNET academic network. https://www.tudelft.nl/mudnet/.

Appendix A. Supplementary data

Supplementary data to this article can be found online at https://doi.org/10.1016/j.marpetgeo.2020.104338.

References

Barbot, E., Dussouillez, P., Bottero, J.Y., Moulin, P., 2010. Coagulation of bentonite suspension by polyelectrolytes or ferric chloride: floc breakage and reformation. Chem. Eng. J. 156 (1), 83–91.
Barnes, H.A., 1995. A review of the slip (wall depletion) of polymer solutions, emulsions and particle suspensions in viscometers: its cause, character, and cure. J. Non-Newtonian Fluid Mech. 56, 221–251.
Barnes, H.A., 1999. The yield stress—a review or 'παντα ρει'—everything flows? J. Non-Newtonian Fluid Mech. 81, 133–178.
Berlamont, J., Ockenden, M., Toorman, E., Winterwerp, J., 1993. The characterisation of cohesive sediment properties. Coast. Eng. 21, 105–128.
Cheng, D.C.-H., 1987. Thixotropy. Int. J. Cosmet. Sci. 9, 151–191.
Coussot, P., 1997. Mudflow Rheology and Dynamics. Routledge, London.
Coussot, P., Tabuteau, H., Chateau, X., Tocquer, L., Ovarlez, G., 2006. Aging and solid or liquid behavior in pastes. J. Rheol. 50, 975–994.
Derec, C., Ducouret, G., Ajdari, A., Lequeux, F., 2003. Aging and nonlinear rheology in suspensions of polyethylene oxide–protected silica particles. Phys. Rev. 67, 061403.
Fischer, C., Plummer, C.J.G., Michaud, V., Bourban, P.-E., Månson, J.-A.E., 2007. Pre- and post-transition behavior of shear-thickening fluids in oscillating shear. Rheol. Acta 46, 1099–1108.
Galindo-Rosales, F.J., Rubio-Hernández, F.J., Velázquez-Navarro, J.F., 2009. Shear-thickening behavior of Aerosil® R816 nanoparticles suspensions in polar organic liquids. Rheol. Acta 48, 699–708.
Goudoulas, T.B., Germann, N., 2016. Viscoelastic properties of polyacrylamide solutions from creep ringing data. J. Rheol. 60, 491–502.
Habermann, C., Wurpts, A., 2008. Occurrence, behaviour and physical properties of fluid mud. In: Proceedings des Chinese-German Joint Symposium on Hydraulic and Ocean Engineering (JOINT2008), Darmstadt.
Hammadi, L., Boudjenane, N., Belhadri, M., 2014. Effect of polyethylene oxide (PEO) and shear rate on rheological properties of bentonite clay. Appl. Clay Sci. 99, 306–311.
He, W., Nan, J., Li, H., Li, S., 2012. Characteristic analysis on temporal evolution of floc size and structure in low-shear flow. Water Res. 46, 509–520.
Ilstad, T., Elverhøi, A., Issler, D., Marr, J.G., 2004. Subaqueous debris flow behaviour and its dependence on the sand/clay ratio: a laboratory study using particle tracking. Mar. Geol. 213, 415–438.
ISO, 1995. Soil Quality: Determination of Organic and Total Carbon after Dry Combustion (Elementary Analysis). ISO.
Janssens, W., Goderis, B., Van Puyvelde, P., 2017. The effect of shear history on urea containing gliadin solutions. J. Polym. Eng. 861.
Joshi, Y.M., Reddy, G.R.K., Kulkarni, A.L., Kumar, N., Chhabra, R.P., 2007. Rheological behaviour of aqueous suspensions of laponite: new insights into the ageing phenomena. Proc. Math. Phys. Eng. Sci. 464, 469–489.
Kanai, H., Amari, T., 1993. Strain-thickening transition in ferric-oxide suspensions under oscillatory shear. Rheol. Acta 32, 539–549.
Kanai, H., Navarrete, R., Macosko, C., Scriven, L., 1992. Fragile networks and rheology of concentrated suspensions. Rheol. Acta 31, 333–344.
Khalkhal, F., Carreau, P.J., Ausias, G., 2011. Effect of flow history on linear viscoelastic properties and the evolution of the structure of multiwalled carbon nanotube suspensions in an epoxy. J. Rheol. 55, 153–175.
Kinloch, I.A., Roberts, S.A., Windle, A.H., 2002. A rheological study of concentrated aqueous nanotube dispersions. Polymer 43, 7483–7491.
Malarkey, J., Baas, J.H., Hope, J.A., Aspden, R.J., Parsons, D.R., Peakall, J., Paterson, D.M., Schindler, R.J., Ye, L., Lichtman, I.D., 2015. The pervasive role of biological cohesion in bedform development. Nat. Commun. 6, 6257.
Manning, A.J., Baugh, J.V., Spearman, J.R., Pidduck, E.L., Whitehouse, R.J.S., 2011. The settling dynamics of flocculating mud-sand mixtures: Part 1—empirical algorithm development. Ocean Dynam. 61, 311–350.
Manning, A.J., Baugh, J.V., Spearman, J.R., Whitehouse, R.J.S., 2010. Flocculation settling characteristics of mud: sand mixtures. Ocean Dynam. 60, 237–253.
McMinn, W.A.M., Keown, J., Allen, S.J., Burnett, M.G., 2004. Effect of shear on concentrated hydrous ferric floc rheology. Water Res. 38, 1873–1883.
Mehta, A.J., 1986. Characterization of cohesive sediment properties and transport processes in estuaries. In: Mehta, A.J. (Ed.), Estuarine Cohesive Sediment Dynamics. Springer-Verlag, pp. 290–325.
Mehta, A.J., Manning, A.J., Khare, Y.P., 2014. A note on the Krone deposition equation and significance of floc aggregation. Mar. Geol. 354, 34–39.
Mewis, J., 1979. Thixotropy - a general review. J. Non-Newtonian Fluid Mech. 6, 1–20.
Mewis, J., de Bleyser, R., 1972. Dynamic behavior of thixotropic systems. J. Colloid Interface Sci. 40, 360–369.
Mobuchon, C., Carreau, P.J., Heuzey, M.-C., 2007. Effect of flow history on the structure of a non-polar polymer/clay nanocomposite model system. Rheol. Acta 46, 1045–1056.
Mobuchon, C., Carreau, P.J., Heuzey, M.-C., 2009. Structural analysis of non-aqueous layered silicate suspensions subjected to shear flow. J. Rheol. 53, 1025–1048.
Nie, S., Jiang, Q., Cui, L., Zhang, C., 2020. Investigation on solid-liquid transition of soft mud under steady and oscillatory shear loads. Sediment. Geol. 397, 105570.
Nosrati, A., Addai-Mensah, J., Skinner, W., 2011. Rheology of aging aqueous muscovite clay dispersions. Chem. Eng. Sci. 66, 119–127.
Parsons, D.R., Schindler, R.J., Hope, J.A., Malarkey, J., Baas, J.H., Peakall, J., Manning, A.J., Ye, L., Simmons, S., Paterson, D.M., Aspden, R.J., Bass, S.J., Davies, A.G., Lichtman, I.D., Thorne, P.D., 2016. The role of biophysical cohesion on subaqueous bed form size. Geophys. Res. Lett. 43, 1566–1573.
Paterson, D.M., Crawford, R.M., Little, C., 1990. Subaerial exposure and changes in the stability of intertidal estuarine sediments. Estuarine. Coast. Shelf Sci. 30, 541–556.
Paterson, D.M., Hagerthey, S.E., 2001. Microphytobenthos in constrasting coastal ecosystems: biology and dynamics. In: Reise, K. (Ed.), Ecological Comparisons of Sedimentary Shores. Springer Berlin Heidelberg, Berlin, Heidelberg, pp. 105–125.
Phuoc, T.X., Wang, P., McIntyre, D., Shadle, L., 2014. Synthesis and characterization of a thixotropic coal–water slurry for use as a liquid fuel. Fuel Process. Technol. 127, 105–110.
Qu, J.P., Chen, H.Z., Liu, S.R., Tan, B., Liu, L.M., Yin, X.C., Liu, Q.J., Guo, R.B., 2013. Morphology study of immiscible polymer blends in a vane extruder. J. Appl. Polym. Sci. 128, 3576–3585.
Raghavan, S.R., Khan, S.A., 1995. Shear-induced microstructural changes in flocculated suspensions of fumed silica. J. Rheol. 39, 1311–1325.
Roussel, N., Ovarlez, G., Garrault, S., Brumaud, C., 2012. The origins of thixotropy of fresh cement pastes. Cement Concr. Res. 42, 148–157.
Schindler, R.J., Parsons, D.R., Ye, L., Hope, J.A., Baas, J.H., Peakall, J., Manning, A.J., Aspden, R.J., Malarkey, J., Simmons, S., Paterson, D.M., Lichtman, I.D., Davies, A.G., Thorne, P.D., Bass, S.J., 2015. Sticky stuff: redefining bedform prediction in modern and ancient environments. Geology 43, 399–402.
Schoukens, G., Mewis, J., 1978. Nonlinear rheological behaviour and shear-dependent structure in colloidal dispersions. J. Rheol. 22, 381–394.
Shakeel, A., Kirichek, A., Chassagne, C., 2019. Is density enough to predict the rheology of natural sediments? Geo Mar. Lett. 39, 427–434.
Shakeel, A., Kirichek, A., Chassagne, C., 2020. Rheological analysis of mud from port of Hamburg, Germany. J. Soils Sediments 1–10.
Soulsby, R.L., Manning, A.J., Spearman, J., Whitehouse, R.J.S., 2013. Settling velocity and mass settling flux of flocculated estuarine sediments. Mar. Geol. 339, 1–12.
Spearman, J.R., Manning, A.J., Whitehouse, R.J.S., 2011. The settling dynamics of flocculating mud and sand mixtures: part 2—numerical modelling. Ocean Dynam. 61, 351–370.
Spencer, K.L., Manning, A.J., Droppo, I.G., Leppard, G.G., Benson, T., 2010. Dynamic interactions between cohesive sediment tracers and natural mud. J. Soils Sediments 10, 1401–1414.
Sun, G., Zhang, J., 2015. Structural breakdown and recovery of waxy crude oil emulsion gels. Rheol. Acta 54, 817–829.
Van Den Tempel, M., 1979. Rheology of concentrated suspensions. J. Colloid Interface Sci. 71, 18–20.
Whitby, C.P., Garcia, P.C., 2014. Time-dependent rheology of clay particle-stabilised emulsions. Appl. Clay Sci. 96, 56–59.
Whitehouse, R., Manning, A., 2007. Mixing it: How Marine Mud and Sand Interact. Innovation & Research Focus, Institution of Civil Engineering, vol. 71 Thomas Telford Services Ltd, London.
Whitehouse, R., Soulsby, R., Roberts, W., Mitchener, H., 2000. Dynamics of Estuarine Muds: A Manual for Practical Applications. Thomas Telford.
Xiaochun, Y., Zhongwei, Y., Guangjian, H., Zhitao, Y., Baiping, X., 2015. The design and performance of a vane mixer based on extensional flow for polymer blends. J. Appl. Polym. Sci. 132.
Xu, W., Gao, B., Yue, Q., Wang, Y., 2010. Effect of shear force and solution pH on flocs breakage and re-growth formed by nano-Al13 polymer. Water Res. 44, 1893–1899.
Yu, W.Z., Gregory, J., Campos, L., Li, G., 2011. The role of mixing conditions on floc

growth, breakage and re-growth. Chem. Eng. J. 171 (2), 425–430.
Yuan, D.Q., Wang, Y.L., Feng, J., 2014. Contribution of stratified extracellular polymeric substances to the gel-like and fractal structures of activated sludge. Water Res. 56, 56–65.
Yüce, C., Willenbacher, N., 2017. Challenges in Rheological Characterization of Highly Concentrated Suspensions - A Case Study for Screen-Printing Silver Pastes. JoVE, e55377.
Zhao, Y.X., Gao, B.Y., Zhang, G.Z., Phuntsho, S., Wang, Y., Yue, Q.Y., Li, Q., Shon, H.K., 2013. Comparative study of floc characteristics with titanium tetrachloride against conventional coagulants: Effect of coagulant dose, solution pH, shear force and break-up period. Chem. Eng. J. 233, 70–79.